Rapidly clearable $MnCo_2O_4$@PAA as novel nanotheranostic agent for T_1/T_2 bimodal MRI imaging-guided photothermal therapy

Ying Zhao,[a,b] Yang Liu,[a,b] Yinghui Wang,*[,a] Bo Xu,[e] Songtao Zhang,[a] Jianhua Liu,[d] Tianqi Zhang,[d] Longhai Jin,*[,d] Songyan Song,[a] and Hongjie Zhang*[,a,b,c]

a. State Key Laboratory of Rare Earth Resource Utilization, Changchun Institute of Applied Chemistry (CIAC), Chinese Academy of Sciences, Changchun, Jilin, 130022, China.

b. School of Applied Chemistry and Engineering University of Science and Technology of China, Hefei 230026, China.

c. Department of Chemistry, Tsinghua University, Beijing 100084, China.

d. Department of Radiology, The second hospital of Jilin University, Changchun 130041, China.

e. The first hospital of Jilin University, Changchun 130021, China.

E-mail: yhwang@ciac.ac.cn (Y. Wang), jinlonghai@jlu.edu.cn (L. Jin), hongjie@ciac.ac.cn (H. J. Zhang).

Experimental procedures

Chemicals and Reagents: Mn (II) acetate tetrahydrate ($Mn(OAc)_2 \cdot 4H_2O$) and ammonium hydroxide ($NH_3 \cdot H_2O$) were all purchased from Shanghai Aladdin-Reagent (China). Co (II) acetate tetrahydrate ($Co(OAc)_2 \cdot 4H_2O$) was obtained from Guangfu Chemical Reagent Factory (China). Calcein acetoxymethyl ester (Calcein AM), polyacrylic acid (PAA), and propidium iodide (PI) were purchased from Sigma-Aldrich (MO, USA). The CCK-8 was obtained from Changchun Sanbang Pharmaceutical Technology Co (Changchun, China). Other chemicals were purchased from Beijing Chemical Reagent (China).

Preparation of $MnCo_2O_4$@PAA: $Co(OAc)_2 \cdot 4H_2O$ (0.319 g) and $Mn(OAc)_2 \cdot H_2O$ (0.157 g) were dissolved in the mixture of 96 mL of ethanol and 4 mL of deionized water, followed by the addition of 0.5 mL of $NH_3 \cdot H_2O$ at room temperature. Afterward, the mixture was added into Teflon-lined autoclave and placed in a 150 ℃ oven for 1 h. Thereafter, $MnCo_2O_4$ were obtained by centrifugation and washed with ethanol for three times. Then, $MnCo_2O_4$ were added dropwise into deionized water dissolved with PAA and stirred for 24 h. Finally, $MnCo_2O_4$@PAA were purified by dialysis for two days.

Photothermal effect and thermal stability of $MnCo_2O_4$@PAA: Firstly, 1 ml $MnCo_2O_4$@PAA solution with different concentrations (0, 50, 100, 150, 200 μg mL^{-1}) was poured into a 5 ml quartz cuvette. Then, the solution was exposed to an 808 nm laser (1.5 W cm^{-2}), and a thermocouple probe was employed to measure temperature variation every 30 s. At the same time, thermal images was recorded by an infrared thermal imaging camera (FLIR T420, Fluke, USA). Thereafter, the solution was cooled down naturally to the room temperature to evaluate their photothermal stability. All above experiments was repeated for 3 times.

In vitro and in vivo MR imaging: For MR imaging in vitro, different concentrations of $MnCo_2O_4$@PAA (Mn: 0, 0.119, 0.238, 0.475, 0.95, 1.9 mM or Co:0, 0.263, 0.525, 1.05, 2.1, 4.2 mM) were detected by a 3.0 T MRI system (Discovery MR750w, GE, America). Then, $MnCo_2O_4$@PAA (1mg mL^{-1}, 100 μL) were intravenously injected into a U14 tumor-bearing mouse, and the MRI signals was detected before and after injection (2, 24 h).

Cytotoxicity assay and PTT effect of $MnCo_2O_4$@PAA: Non-cancerous mouse fibroblast (L929) cells and human cervix cancer (HeLa) cells were seeded into 96-well plates for 24 h (37 ℃, 5% CO_2). Then, different concentrations of $MnCo_2O_4$@PAA (0, 50, 100, 150 and 200 μg mL^{-1}) was added in it and incubated for another day. Thereafter, the cells were washed with PBS for three times and re-incubated with CCK-8 solution (10% in DMEM). Two hours later, the 96-well plates were put in a plate reader to record the absorbance values at 450 nm. To assess the PTT performance of $MnCo_2O_4$@PAA, HeLa cells were incubated with different concentrations of $MnCo_2O_4$@PAA (0, 50, 100, 150 and 200 μg mL^{-1}) for 24 h. Afterwards, 808 nm laser (1.5 W cm^{-2}) was employed to irradiate cells for 10 min. Finally, the survival rate of HeLa cells was measure by CCK-8 assay.

Anticancer effect of $MnCo_2O_4$@PAA in vivo: The tumor models was made by subcutaneous injection of U14 cells on Kunming mice. Then, the Kunming mice were split up into the following groups: (I) PBS, (II) 808 nm laser, (III) $MnCo_2O_4$@PAA, and (IV) $MnCo_2O_4$@PAA + 808 nm groups. Mice in (I) and (II) groups were intravenously injected with PBS, while mice were injected with $MnCo_2O_4$@PAA (1 mg mL^{-1}, 100 μL) in (III) and (IV) groups. 2 h later, the tumors of mice in (II) and (IV) groups were exposed to 808 nm laser (1.5 W cm^{-2}) for 10 min. And the size of tumor and body weight were recorded every two days during this period. The tumor volume was figured as follow: $V = (\text{Tumor Length}) \times (\text{Tumor Width})^2/2$. On the 15th day, the tumors were dissected to evaluate the therapeutic efficacy.

Biodistribution of $MnCo_2O_4$@PAA: There were three mice in each group, and they were sacrificed at day(s) 0.125, 0.5, 1, 3, 5, 7 and 14 after intravenous injection with $MnCo_2O_4$@PAA. After that, their main organs were harvested and weighed including heart, liver, spleen, lung, kidney, and tumor. Finally, They were dissolved in aqua regia (HNO_3:HCl = 1:3) for two days to determine Co contents.

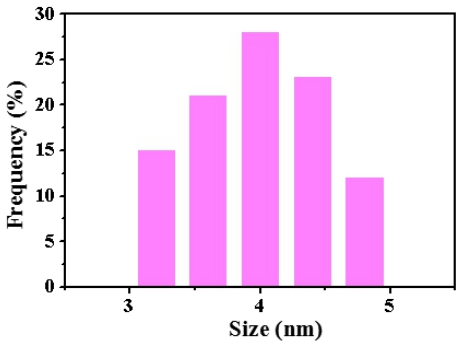

Figure S1. Size distribution histogram of of $MnCo_2O_4$

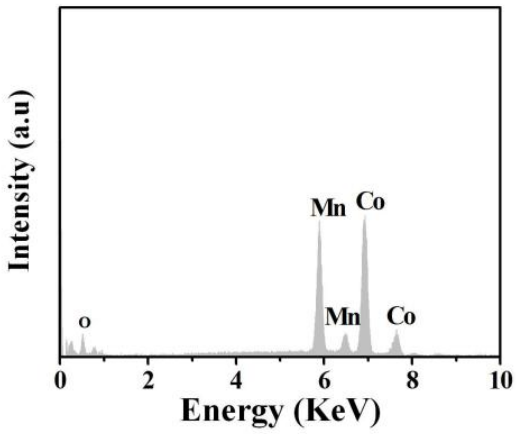

Figure S2. EDS of $MnCo_2O_4$.

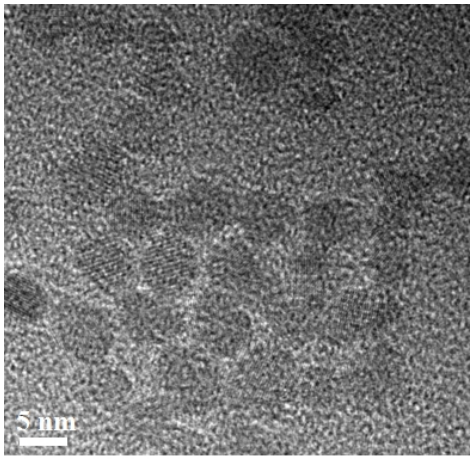

Figure S3. TEM images of $MnCo_2O_4$@PAA.

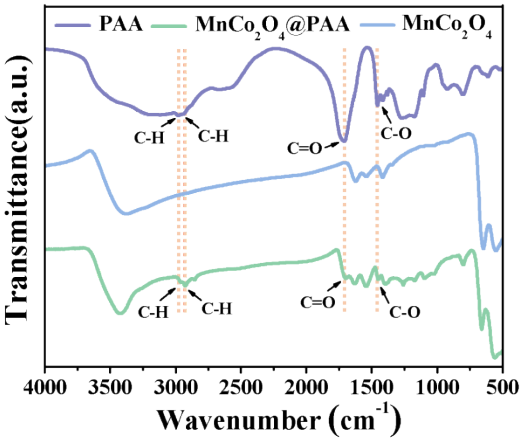

Figure S4. FT-IR spectra of $MnCo_2O_4$, PAA, and $MnCo_2O_4$@PAA.

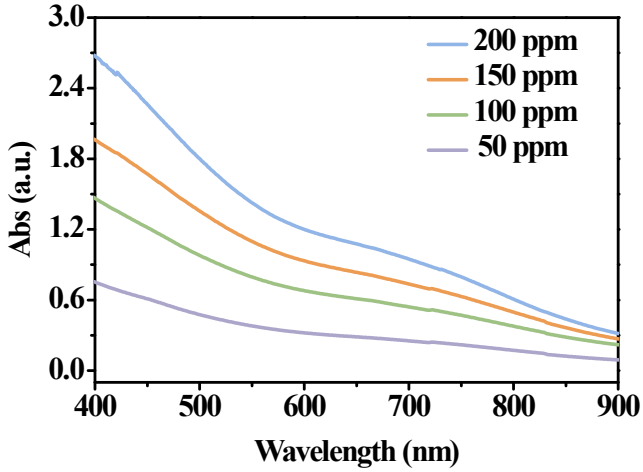

Figure S5. UV-vis absorption spectra of $MnCo_2O_4$ with various concentrations (50, 100, 150, 200 μg mL^{-1}).

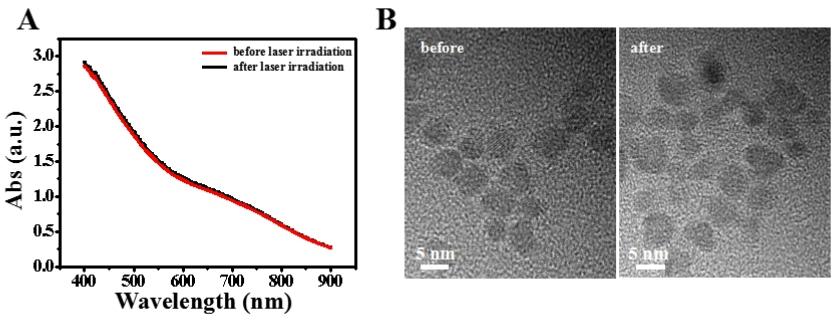

Figure S6. (A) UV-Vis spectrum and (B) morphology of $MnCo_2O_4$@PAA before and after irradiation with 808 nm laser.

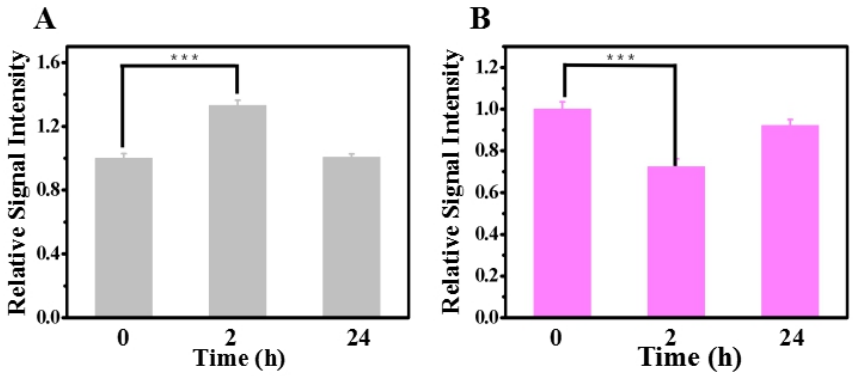

Figure S7. Quantification of (A) T_1-weighted and (B) T_2-weighted MRI signals in tumors after intravenous injection of $MnCo_2O_4$@PAA in vivo, ***$p < 0.001$ (two-tailed t-test).

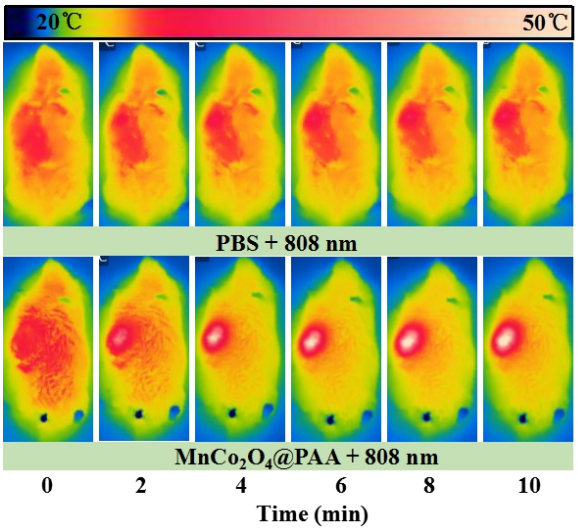

Figure S8. Thermal imaging of U14 tumor-bearing mice.

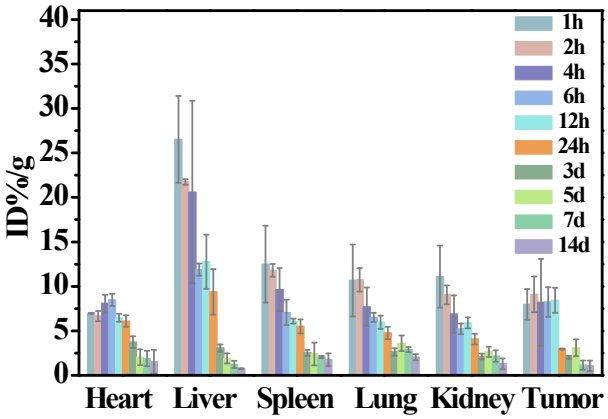

Figure S9. Biodistribution of Mn in the tumor and main organs at different times

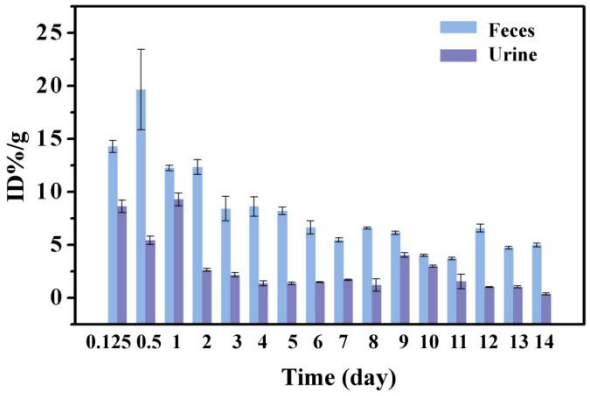

Figure S10. Content of Mn in feces and urine at different time points.

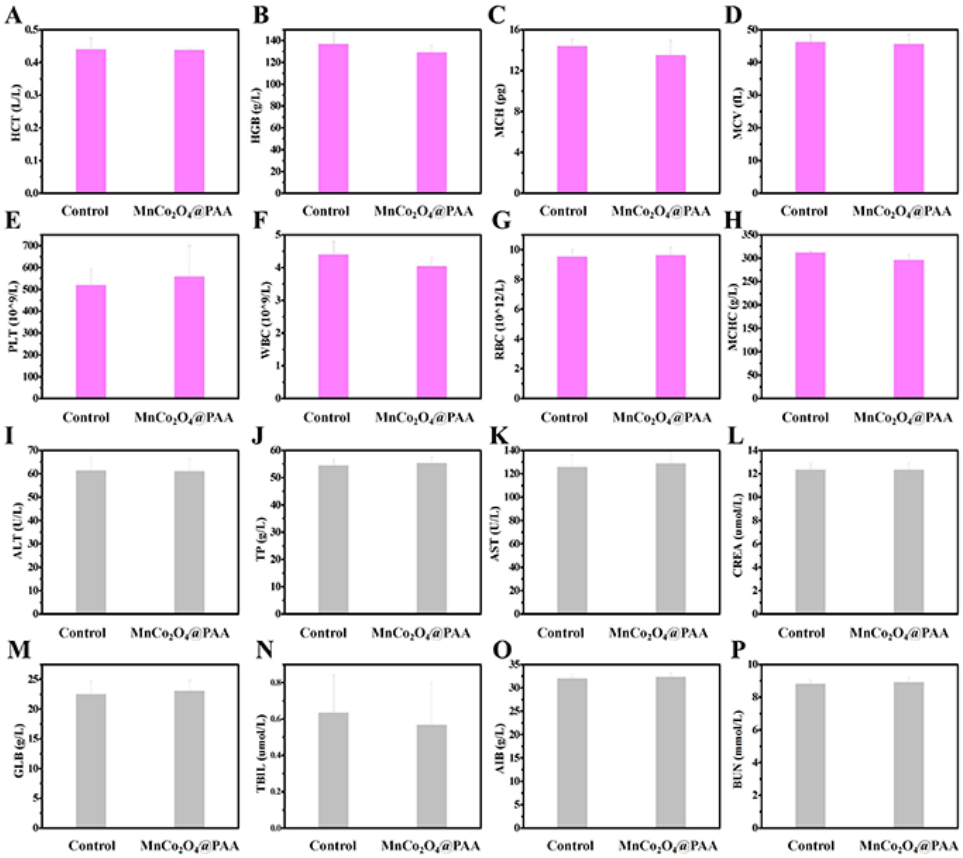

Figure S11. Blood analysis. (a-h) Hematological index and (i-p) biochemical blood analysis of the mice after intravenous injection of $MnCo_2O_4$@PAA at 30 d.